

Microstructures and Corrosion Characteristics of Advanced Fuel Cladding Tubes

150

A alloy, B alloy, C alloy Low Sn Zircaloy-4 D alloy 가 .
TEM 가
가

Abstract

Out-of-pile performances were evaluated for Low Sn Zircaloy-4, A alloy, B alloy, C alloy and D alloy. Observation of microstructure by TEM and analysis of precipitate characteristics were performed to investigate the effect of microstructure on the out-of-pile corrosion behavior of the claddings. Corrosion characteristics of the claddings was evaluated by corrosion test in 360°C loop containing 2.2 ppm LiOH and 650 ppm H₃BO₃, 400°C steam and 360°C 70 ppm LiOH. Mechanical properties of the claddings were examined by tensile test and creep test.

1.

가 , 30%
가
Zr , 1990
가 Zircaloy-4 가
/ , pH 가 , 1
1960 가 Zircaloy-4 가
1). 가 / 가
(Autoclave) 가 가

5 μ m 가 가 가 가

Zr 1990
Zr 가

가 가

2.

Low Sn Zircaloy-4
A alloy, B alloy, C alloy D alloy
TEM as-received 가 ,
가 .
Table 1
25mm , 5% HF + 45% HNO₃ + 50% H₂O
ASTM (G2-88) 360 2.2ppm LiOH
650ppm H₃BO₃ water (Loop), 400 steam 360 70ppm LiOH
270
TEM EDS
TEM 10% HClO₃, 90% C₂H₅OH twin-jet
polishing
0.25mm/min 2.5mm/min 가 ,
150MPa (hoop stress) 가 400
, Ar 가 가
K-type
2 ,
5 .

3.

Fig. 1 A alloy, B alloy, C alloy D alloy as-recieved
 (stress-relieved), (partially recrystallized)
 (recrystallized) as-received
 , A alloy, C alloy D alloy , B alloy
 가
 , Low Sn Zircaloy-4 Fig. 2
 , A alloy , Fig. 3 Fig. 4
 Zr(Fe,Cr)₂가 , -Nb ZrNbFe , B alloy -Nb
 , (Fig. 5). , C alloy D alloy

Table 2

Low Sn Zircaloy-4 가 가
 , Nb 가 Zr
 Nb 가 Zr
 2
 Nb 가
 가 50nm
 가 200nm
 A alloy 2 가 80nm
 , 2
 Fig. 6 가
 360 Loop, 400 360 70ppm LiOH
 , B alloy가 가 , 360 Loop 270
 Sn Zircaloy-4, C alloy , B alloy , D alloy, A alloy, Low
 50 가 ,
 가 360
 B alloy 가 ,
 가 가 ,
 , B alloy 2), B alloy
 Optimized Zircaloy-4 , 6 63GWD/MTU
 가 27 μm 가

400 D alloy가 가 , Low Sn Zircaloy-4, B alloy, A alloy, C alloy . D alloy, Low Sn Zircaloy-4 B alloy 270 가 , A alloy C alloy

alloy 가 D alloy , 270 가 3 가 C

D alloy BR-2 () 30GWD/MTU 15 μ m , Low Sn Zircaloy-4

McGuire unit 1 3 D alloy 가 Low Sn Zircaloy-4 39GWD/MTU ³⁾

PWR ⁴⁾ D alloy D alloy , Kansai Ohi unit 4 Zircaloy-4 가 가

360 70ppm LiOH A alloy 가 가 가 70ppm LiOH A alloy 가 가 가 Low Sn Zircaloy-4 45 가 가 가 가 180 가 가 가 C alloy D alloy 210 가 가 B alloy, D alloy, C alloy, Low Sn Zircaloy-4

⁵⁾ A alloy Zircaloy-4 LiOH Zircaloy-4 3-10 A alloy 가 Zircaloy-4

가 Zircaloy-4 North Anna 1 ⁶⁾ 3 54.7GWD/MTU 가 A alloy

Zircaloy-4 Fig. 7 5 B alloy B alloy 4

Zry-4 400°C 2 A alloy A alloy Low Sn Low Sn Zry-4

(Stress relieved) TEM A alloy가 Low Sn Zry-4 가 가

가 400 , 150MPa A alloy, B alloy Low Sn Zircaloy-4 Fig. 8

, B alloy가 A alloy 가 , Low Sn Zircaloy-4

B alloy ²⁾ 1-5 $\times 10^{21}$ n/cm² 0.5% Optimized Zircaloy-4 B alloy

Optimized Zircaloy-4 2%

4.

A alloy, B alloy, C alloy Low Sn Zircaloy-4 가
D alloy TEM
가
가

- 1) F. Garzarolli, R. P. Bodmer, H. Stehle and D. Trapp-Pritsching, Proceedings of the 1985 International Topical Meeting on LWR Fuel Performance, Orlando, 1985, pp. 3-55.
- 2) J. -P. Mardon, D. Charquet and J. Senevat, Zirconium in the Nuclear Industry: Twelfth International Symposium, ASTM STP 1354, G. P. Sabol and G. D. Moan, Eds., American Society for Testing and Materials, West Conshohocken, PA, 2000, pp. 505-524.
- 3) K. Yamate, A. Oe, M. Hayashi, T. Okamoto, H. Anada and S. Hagi, Proceedings of the 1997 International Topical Meeting on LWR Fuel Performance, 1997, pp. 318-325.
- 4) K. Goto, S. Matsumoto, T. Murata, H. Anada and H. Abe, Proceedings of the 2000 International Topical Meeting on LWR Fuel Performance, Park City, Utah, April 10-13, 2000.
- 5) G. P. Sabol, R. J. Comstock, R. A. Weiner, P. Larouer and R. N. Stanutz, Zirconium in the Nuclear Industry: Tenth International Symposium, ASTM STP 1245, A. M. Garde and E. R. Bradley, Eds., American Society for Testing and Materials, Philadelphia, 1994, pp. 724-744.
- 6) R. J. Comstock, G. Schoenberger and G. P. Sabol. Zirconium in the Nuclear Industry: Eleventh International Symposium, ASTM STP 1295, E. R. Bradley and G. P. Sabol, Eds., American Society for Testing and Materials, Philadelphia, 1996, pp. 710-725.

Table 1. Chemical compositions of the foreign advanced Zr claddings (wt.%).

	Nb	Sn	Fe	Cr	Ni	O	Zr
A alloy	1	1	0.1				Bal.
B alloy	1					0.12	Bal.
C alloy	0.5	0.8	0.2	0.1			Bal.
D alloy	0.1	1.0	0.27	0.16	0.01		Bal.
Low Sn Zry-4		1.2	0.2	0.1			Bal.

Table 2. Characteristics of intermetallic compounds precipitated in the foreign advanced Zr claddings used in this study.

	Precipitate type	Crystal structure
A alloy	-Nb ZrNbFe	bcc hcp
B alloy	-Nb	bcc
C alloy	Zr(Fe,Cr) ₂	hcp
D alloy	Zr(Fe,Cr) ₂ Zr ₂ (Fe,Ni)	hcp hcp
Low Sn Zry-4	Zr(Fe,Cr) ₂	hcp

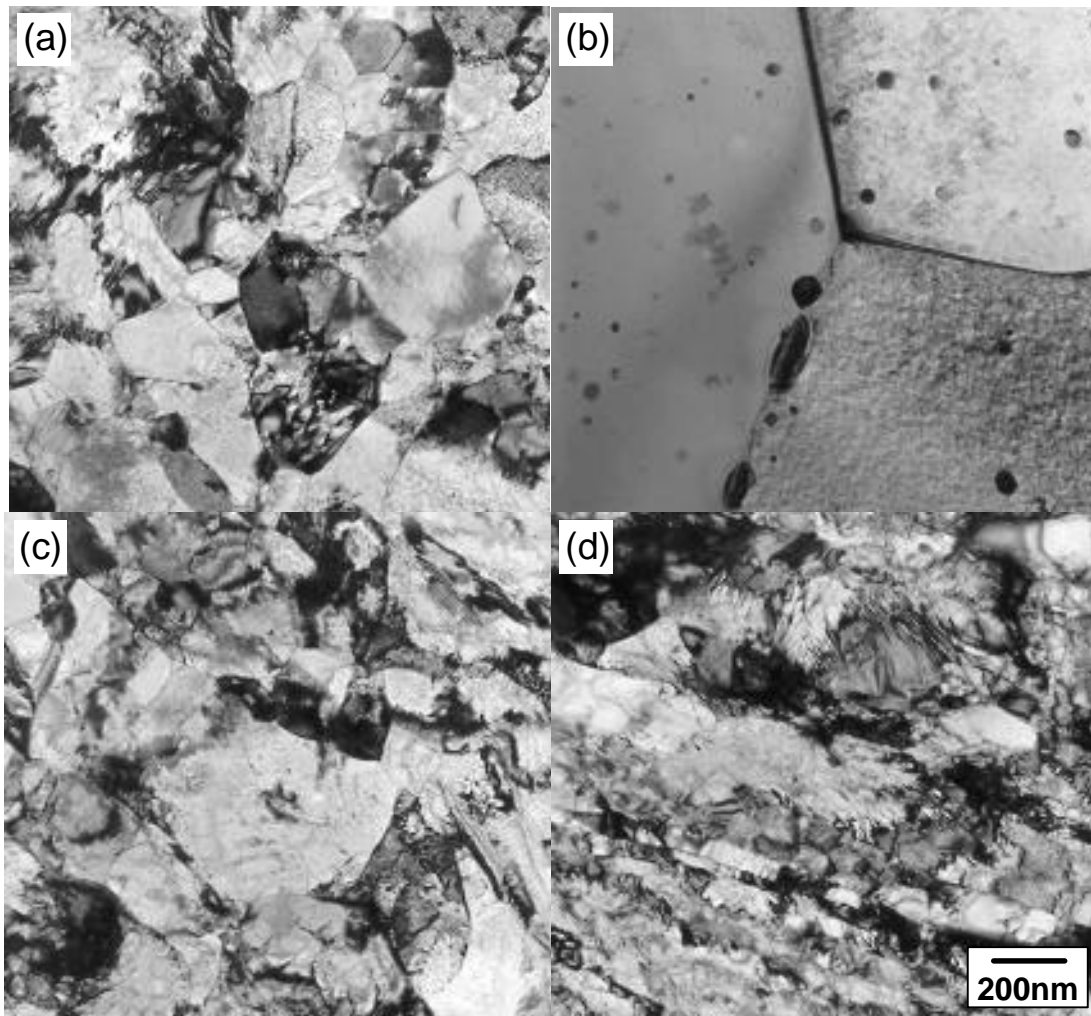


Fig. 1. TEM microstructures of as-received (a) A alloy, (b) B alloy, (c) C alloy and (d) D alloy claddings.

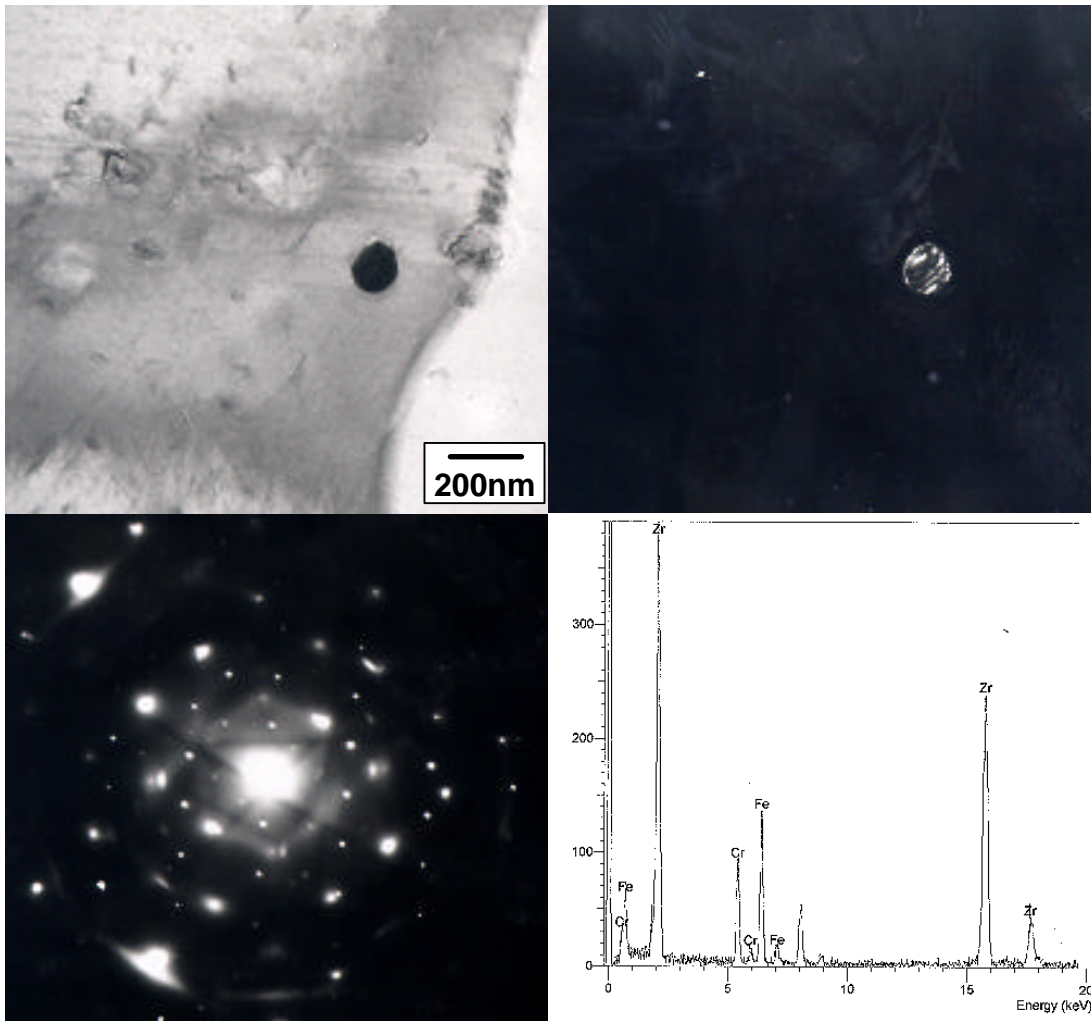


Fig. 2. Bright field image, dark field image, selected area diffraction pattern and EDS spectrum on $Zr(Fe,Cr)_2$ in Low Sn Zircaloy-4.

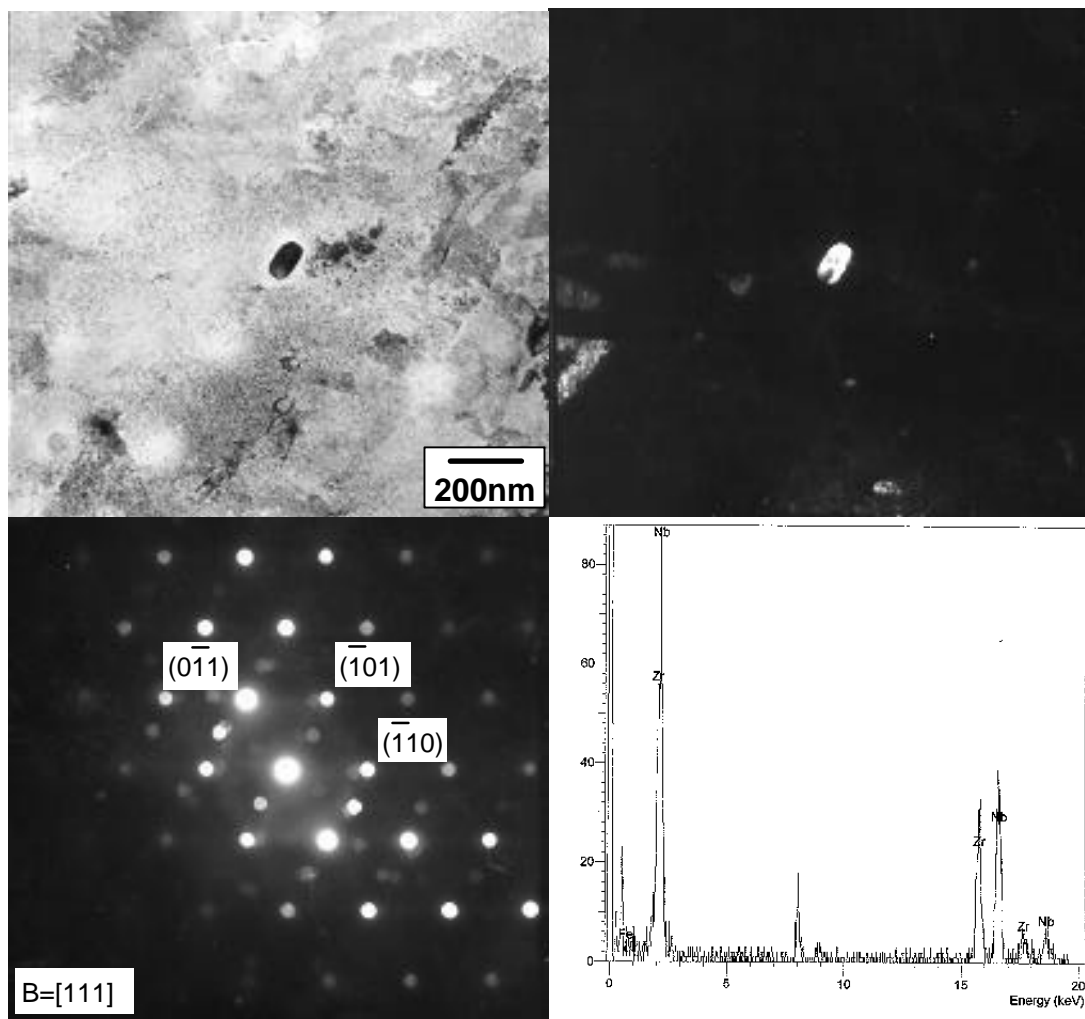


Fig. 3. Bright field image, dark field image, selected area diffraction pattern and EDS spectrum on β -Nb in A alloy.

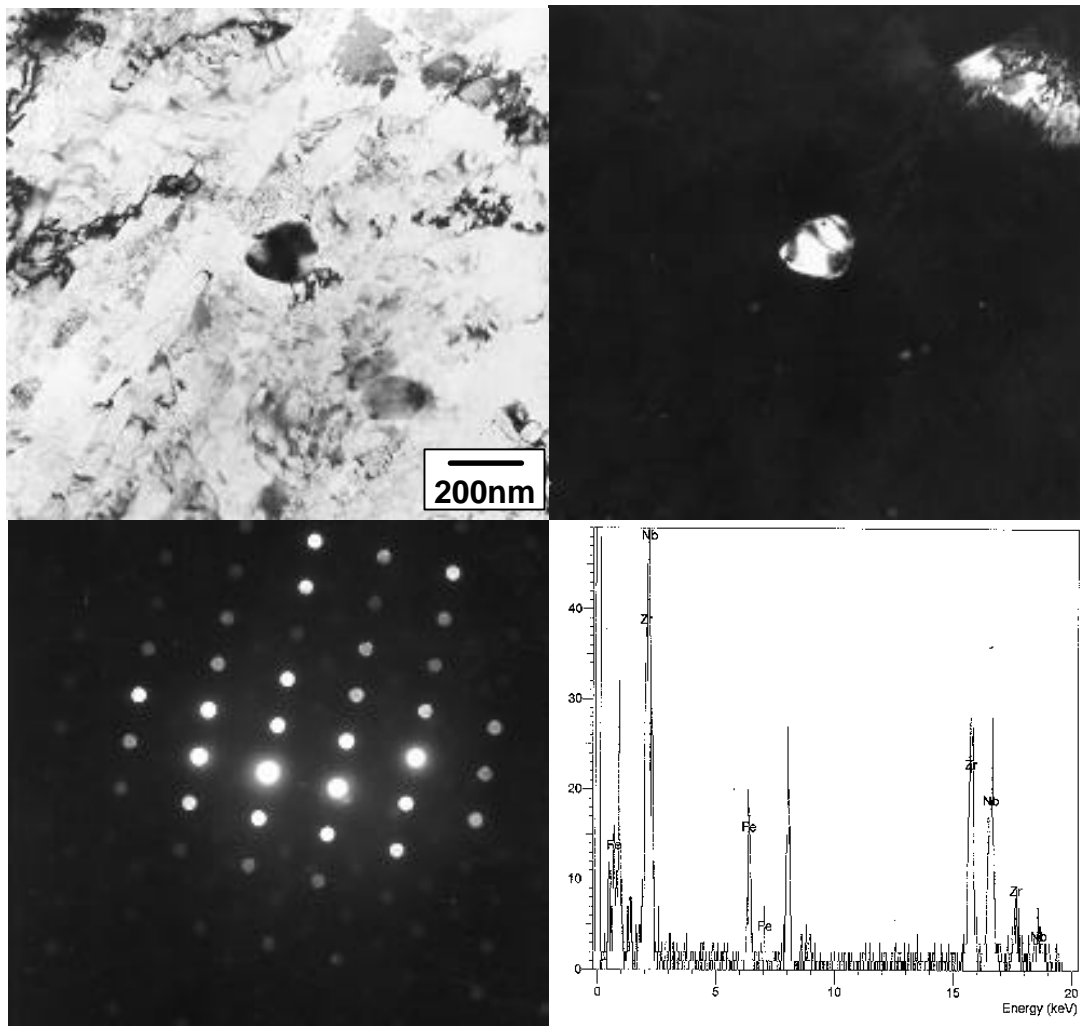


Fig. 4. Bright field image, dark field image, selected area diffraction pattern and EDS spectrum on ZrNbFe precipitate in A alloy.

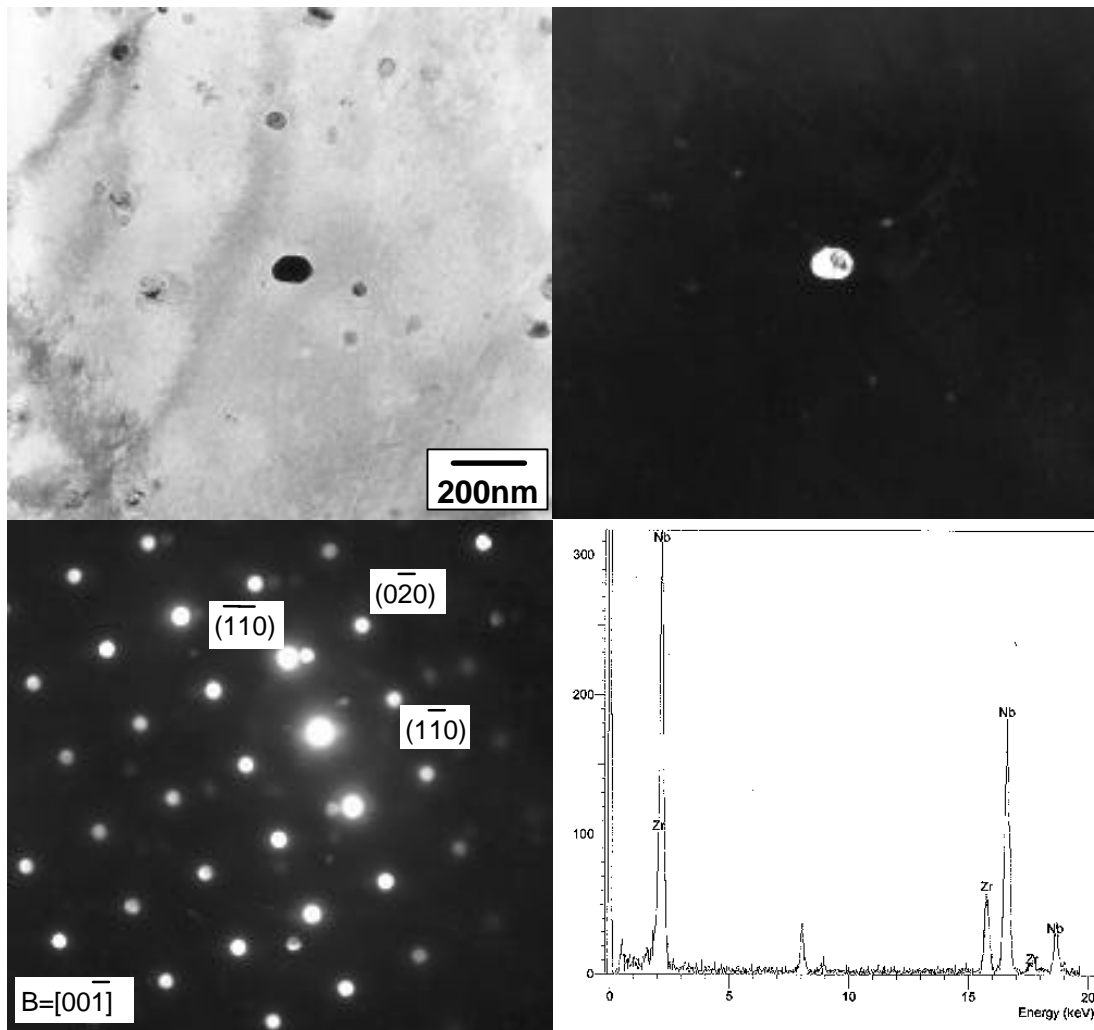


Fig. 5. Bright field image, dark field image, selected area diffraction pattern and EDS spectrum on β -Nb in B alloy.

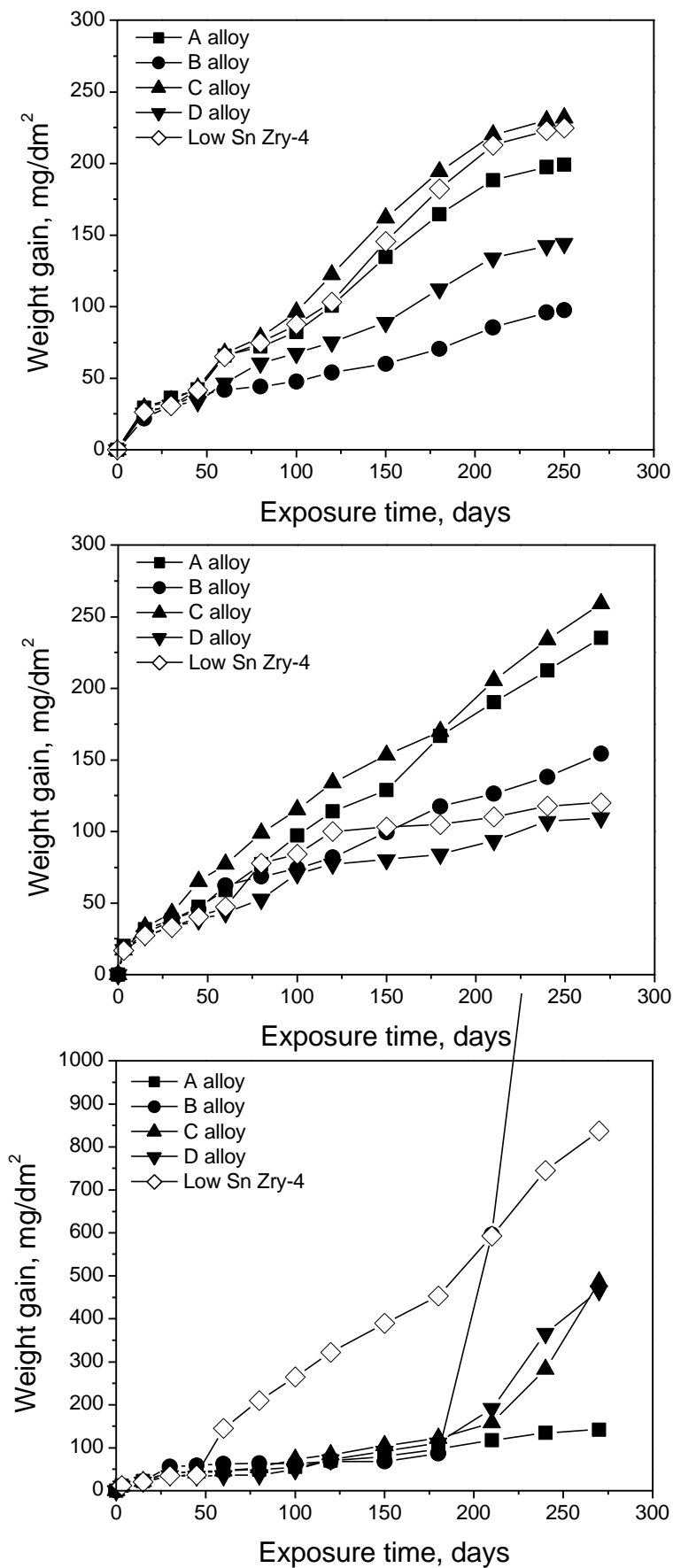


Fig. 6. Corrosion behavior of A alloy, B alloy, C alloy, D alloy and Low Sn Zircaloy-4 claddings in (a) Loop at 360°C, (b) steam at 400°C and (c) 70ppm LiOH at 360°C.

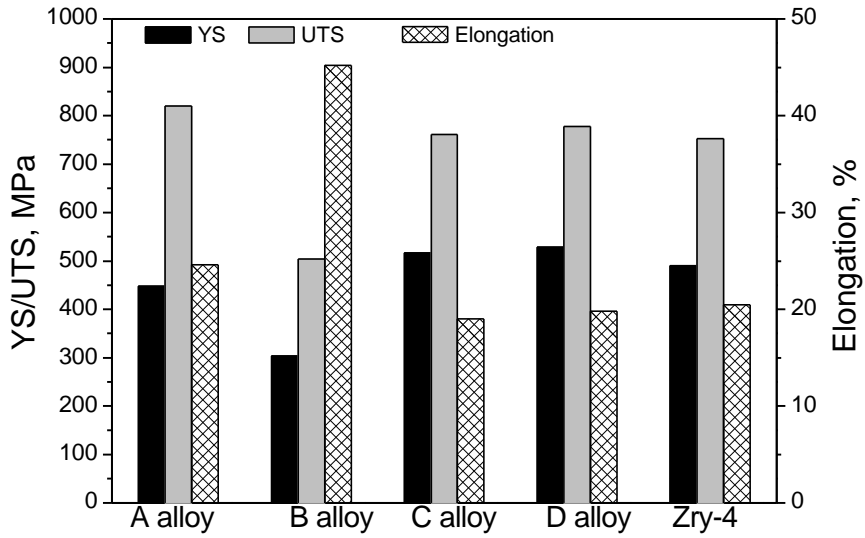


Fig. 7. Tensile properties of A alloy, B alloy, C alloy, D alloy and Low Sn Zircaloy-4 claddings at room temperature.

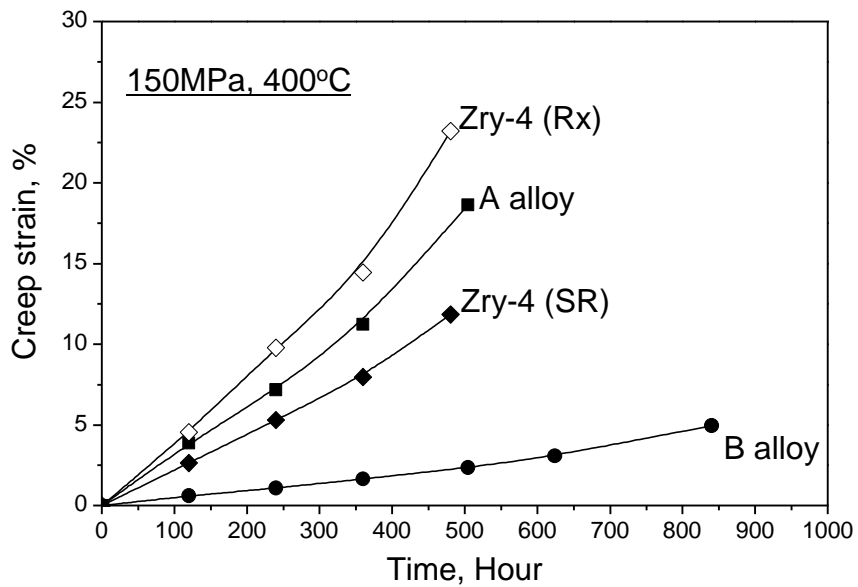


Fig. 8. Creep properties of A alloy, B alloy, C alloy, D alloy and Low Sn Zircaloy-4 claddings.